Geophysical Research Letters

RESEARCH LETTER
10.1029/2019GL086061

$^{10}Be/^{9}Be$ Ratios Reveal Marine Authigenic Clay Formation

A. Bernhardt[1], M. Oelze[2], J. Bouchez[3], F. von Blanckenburg[4,1], M. Mohtadi[5], M. Christl[6], and H. Wittmann[4]

[1]Institute of Geological Sciences, Freie Universitaet Berlin, Berlin, Germany, [2]GFZ German Research Centre for Geosciences, Inorganic and Isotope Geochemistry, Potsdam, Germany, [3]Institut de physique du globe de Paris, Université de Paris, CNRS, Paris, France, [4]GFZ German Research Centre for Geosciences, Earth Surface Geochemistry, Potsdam, Germany, [5]MARUM-Center for Marine Environmental Sciences, Bremen University, Bremen, Germany, [6]Laboratory of Ion Beam Physics, Department of Physics, ETH Zurich, Zurich, Switzerland

Abstract As reverse weathering has been shown to impact long-term changes in atmospheric CO_2 levels, it is crucial to develop quantitative tools to reconstruct marine authigenic clay formation. We explored the potential of the beryllium (Be) isotope ratio ($^{10}Be/^{9}Be$) recorded in marine clay-sized sediment to track neoformation of authigenic clays. The power of such proxy relies on the orders-of-magnitude difference in $^{10}Be/^{9}Be$ ratios between continental Be and Be dissolved in seawater. On marine sediments collected along a Chilean margin transect we chemically extracted reactive phases and separated the clay-sized fraction to compare the riverine and marine $^{10}Be/^{9}Be$ ratio of this fraction. $^{10}Be/^{9}Be$ ratios increase fourfold from riverine to marine sediment. We attribute this increase to the incorporation of Be high in $^{10}Be/^{9}Be$ from dissolved biogenic opal, which also serves as a Si-source for the precipitation of marine authigenic clays. $^{10}Be/^{9}Be$ ratios thus sensitively track reverse-weathering reactions forming marine authigenic clays.

Plain Language Summary Clay minerals can form on land by the chemical breakdown of rock-forming minerals, but clays can also form in the ocean. When clay formation takes place in the ocean, CO_2 is released. To date, there is no method that can easily measure the amount of clay minerals formed in the ocean. We used two isotopes of the same element, beryllium (Be), with the atomic mass of 9 and 10 to test whether this isotope system can be used to measure marine clay formation. The abundance of these isotopes differs majorly on land and in the ocean. We measured beryllium isotopes in river sediment and ocean-bottom sediment offshore the Chile coast and compared the ratios of the isotopes ($^{10}Be/^{9}Be$). The ratio is four times higher in ocean sediment, when compared to river sediment. We interpret this increase to be due to the formation of clay minerals in the ocean, which include the high $^{10}Be/^{9}Be$ ratio during their formation. We conclude that the beryllium-isotope system can be used to measure the formation of even very small amounts (less than 2%) of marine clay minerals. This is important, as the clay-forming chemical reactions release CO_2 which has a long-term effect on global climate.

Key Points:
- We explored the potential of the beryllium isotope ratio to track neoformation of marine authigenic clays
- Beryllium isotope ratios increase fourfold from riverine to marine sediment due to the presence of marine Be incorporated in authigenic clay
- Beryllium isotope ratios sensitively track reverse-weathering reactions forming marine authigenic clays

Supporting Information:
- Supporting Information S1

Correspondence to:
A. Bernhardt,
anne.bernhardt@fu-berlin.de

Citation:
Bernhardt, A., Oelze, M., Bouchez, J., von Blanckenburg, F., Mohtadi, M., Christl, M., & Wittmann, H. (2020). $^{10}Be/^{9}Be$ ratios reveal marine authigenic clay formation. *Geophysical Research Letters*, *47*, e2019GL086061. https://doi.org/10.1029/2019GL086061

Received 6 NOV 2019
Accepted 21 DEC 2019
Accepted article online 3 JAN 2020

1. Introduction

Reverse weathering has been recently recognized as an important factor of the ocean alkalinity balance, as HCO_3^- dissolved in seawater is converted into CO_2 which is released back into the atmosphere with implications for global climate (Dunlea et al., 2017; Isson & Planavsky, 2018). During reverse-weathering reactions, neoformation of marine authigenic clays can occur when amorphous silica, aluminosilicates, and hydroxides react to form cation-Al silicates (the authigenic clays), CO_2, and H_2O (Mackenzie & Garrels, 1966; Mackin & Aller, 1984, 1986; Michalopoulos & Aller, 1995, 2004); however, not all authigenic clays are Al-bearing (Tosca et al., 2016). Despite the importance of this phenomenon for the long-term evolution of the ocean chemistry and atmospheric CO_2, unambiguous proxies are still lacking to detect and quantify reverse-weathering reactions, mostly because marine authigenic clays are difficult to distinguish from detrital material by sediment geochemistry or mineralogical analyses (Rahman et al., 2016).

Beryllium is likely to be involved in the formation of these authigenic clays as a trace element. The stable isotope of beryllium, ^{9}Be, is released from bedrock during weathering and introduced to the ocean in the dissolved form where it mixes with the dissolved cosmogenic and radioactive nuclide ^{10}Be (meteoric). Meteoric ^{10}Be is produced via interactions of high-energy cosmic radiation with target nuclei in the atmosphere and is delivered to the Earth surface by atmospheric deposition (Brown, Edmond, et al., 1992). Almost all ^{9}Be

dissolved in the oceans is delivered by rivers, whereas almost all meteoric ^{10}Be is sourced from atmospheric precipitation (Brown, Measures, et al., 1992), such that the concentrations of dissolved ^{10}Be and resulting dissolved $^{10}Be/^{9}Be$ ratios increase from ~1×10^{-9} to 1×10^{-8} in the rivers to >4×10^{-8} in the oceans (von Blanckenburg & Bouchez, 2014, and references therein). This increase occurs in a transition zone along the ocean margin where the width of this zone depends on ocean-surface currents (Igel & von Blanckenburg, 1999). When precipitated into the authigenic phase of marine sediment, consisting of Fe-Mn-oxyhydroxides, biogenic opal, and neo-formed clay, the $^{10}Be/^{9}Be$ ratio of the overlying water column is preserved (Bourlès et al., 1989; Kusakabe & Ku, 1984; von Blanckenburg et al., 1996). This ratio has been applied as a silicate-weathering proxy at a global ocean-basin scale (Rugenstein et al., 2019; von Blanckenburg et al., 2015; von Blanckenburg & Bouchez, 2014; Willenbring & von Blanckenburg, 2010), to reconstruct past events of ice melting at a regional scale (Simon, Thouveny, Bourles, Nuttin, et al., 2016; Valletta et al., 2018) and to constrain the chronology of marine sediment archives (Bourlès et al., 1989), growth rates of manganese crusts (Segl et al., 1984), and ^{10}Be-production changes resulting from variations of Earth's magnetic field (e.g., Carcaillet et al., 2004; Christl et al., 2003; Knudsen et al., 2008; Ménabréaz et al., 2012, 2014; Simon, Thouveny, Bourlès, Valet, et al., 2016; Simon et al., 2018). When seawater Be is incorporated into neo-formed authigenic clays during marine diagenesis, and these clays are added to the clay-sized detrital sediments, an increase in the $^{10}Be/^{9}Be$ ratio after their deposition in the ocean will result.

In this study, we evaluate this hypothesis through the comparison of the mineralogical and elemental composition, as well as of the $^{10}Be/^{9}Be$ isotope ratio of the clay-sized sediment fraction (of which all the Fe-Mn-oxyhydroxide component was removed by sequential extractions) from three terrestrial river catchments located in Chile, and from corresponding marine surface sediment located at four sites along a transect offshore these catchments. In a previous study, Wittmann et al. (2017) extracted the Fe-Mn oxyhydroxide fraction of the marine authigenic phase from the same sample sites. This extracted fraction is hereafter called the "reactive" phase, termed $[^{10}Be]_{reac}$ ([] denote concentrations) and consists mainly of amorphous Fe-Al oxyhydroxides and reactive Fe-Mn surfaces. The concentration of $^{10}Be_{reac}$ of marine surface sediment increased greater than tenfold compared to the contributing river sediments (Wittmann et al., 2017), whereas the corresponding ^{9}Be concentration ($[^{9}Be]_{reac}$) remained roughly constant. This rapid increase in $[^{10}Be]_{reac}$ was interpreted as being related to the growth of authigenic rims on substrate particles through coprecipitation incorporating Be with a high open-ocean $^{10}Be/^{9}Be$ signature only 30 km from the coast. Thus, the inner authigenic rim preserved the $^{10}Be/^{9}Be$ characteristic of continental erosion, whereas the outer rim incorporates Be with an open-ocean $(^{10}Be/^{9}Be)_{reac}$ ratio (Wittmann et al., 2017). In this study we test whether the clay-sized sediment fraction contains Be that either preserves a $^{10}Be/^{9}Be$ ratio representing terrestrial erosion or records marine authigenic clay formation. We show that such pattern of $^{10}Be/^{9}Be$ increase (Wittmann et al., 2017) also applies to the clay-sized component of river and offshore sediments and explore the consequences of this finding for the use of the $^{10}Be/^{9}Be$ proxy as a tracer of authigenic clay formation in the ocean.

2. Study Area and Sampling Strategy

We use the same samples processed in Wittmann et al. (2017), including (1) detrital sediment from three rivers (Biobío, Lebu, Yani) that drain into the Pacific Ocean in central Chile and (2) marine surface sediment offshore central Chile from a coast-perpendicular transect located at 37.4°S of four multicorer sediment cores (MUCs) (RV-Sonne cruise SO-156, Hebbeln and Shipboard Scientists, 2001; Figure 1, Table S1). In this area, submarine weathering of reactive silicate minerals occurs, which are abundant along the Central Chilean margin (Scholz et al., 2013).

The river sediment samples were taken close to the outlets of the Lebu, Yani, and Biobío rivers. To ensure sampling of representative material of the entire river catchment, we sampled about 1 kg of clastic riverine sediment (a mix of clays, silt, and sand) from active river banks. Amalgamated samples were taken from a radius of several tens of meters. We avoided recent landslide and organic-rich material. Marine samples were taken by a multicorer ("MUC") to obtain undisturbed samples of the uppermost two centimeters of sediment. Marine MUC sites 1–3 are located on the continental slope offshore Chile, where downslope sediment transport should dominate. Site MUC 4 is located at the western margin of the subduction trench. The Gunther undercurrent moves material southwestward along the shelf, before it

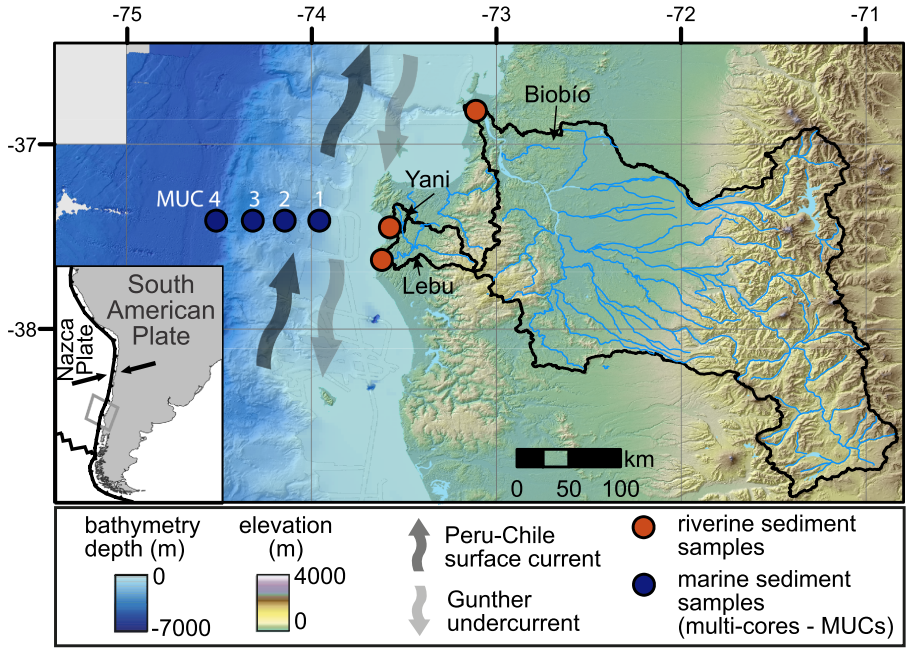

Figure 1. Map of the study area showing terrestrial river sample locations and marine surface sediment sampling sites (MUCs).

sweeps sediment onto the continental slope (Bernhardt et al., 2016). However, little sediment from north of the Biobío River should reach the MUC sites, as the Biobío submarine canyon connects to the river mouth (e.g., Bernhardt et al., 2015; Figure 1) and northward-derived sediment should be funneled through the canyon toward the trench. Mineralogical composition of terrestrial and marine sediment samples shows little differences, suggesting direct transfer from riverine sources to marine depositional sites (Wittmann et al., 2017). Hence, most of the terrestrial sediment reaching the MUC sites is probably derived from the Biobío River due to its large catchment size with minor contributions of the Lebu and Yani catchments. This hypothesis is further tested using mineralogical analyses, combined with Sr and Nd isotope measurements (Supporting Information S1).

3. Methods

3.1. Sequential Extractions

For the chemical extraction of meteoric ^{10}Be, the fine-grained portions of the river sediment and the marine surface sediments (MUCs) are treated identically and prepared as described in Wittmann et al. (2017). The chemical procedures for the separation of Be-bearing phases are modified from Tessier et al. (1979), Bourlès et al. (1989), and Wittmann et al. (2012) and involve step-wise chemical leaching of the sediment resulting in the selective removal of the following phases:

1. the exchangeable ^{10}Be (ex fraction),
2. "reactive" phases (reac fraction) consisting of

   (2a) amorphous Al-Mn-Fe-(hydr-)-oxides (am-ox fraction)
   (2b) crystalline Al-Mn-Fe-(hydr-)-oxides (x-ox fraction),
3. the organic phase (org fraction),
4. biogenic amorphous silica (opal fraction),
5. the residual fraction (min-fraction). The min-fraction is separated into a clay-sized fraction and the remaining coarser silicate residual (clay-sized + sil = min fraction).

Step 1 removes Be adsorbed to surficial exchangeable sites by adding $MgCl_2$ to the sample. During step 2, some authigenic mineral phases, such as carbonates and amorphous and crystalline Al-Fe-Mn (oxy)hydroxides, are selectively removed by a combined weak hydrochloric acid (am-ox) and hydroxylamine-

hydrochloride (x-ox) extraction. Subsequently, the samples are treated during step 3 with a combination of 0.01 M nitric acid and 10 M hydrogen peroxide to extract the organic phase (org fraction). Step 4 removes biogenic amorphous silica by leaching the samples with NaOH (opal fraction) (Foster, 1953; Sauer et al., 2006). All leached solutions are evaporated and brought up in 3 M nitric acid after treatment with aqua regia. Step 5 involves the mechanical separation of remaining min fractions by ultrasonic shaking, centrifuging, and extraction by pipetting into a clay-sized fraction and the sil fraction. These fractions are digested using mixtures of hydrofluoric acid and aqua regia and brought up in 3 M nitric acid.

3.2. Analytical Procedures

To assure that the source of the marine sediments at the MUC sites was effectively the sampled rivers, we performed X-ray diffraction (XRD) and Sr-Nd isotope analyses. Details and results are reported in the Supporting Information (Figures S1 and S2).

From all leachates and the final clay-sized and sil fractions, aliquots of the 3 M nitric acid were set aside for the analysis of ^{9}Be concentrations and major element composition, which was measured by an optical emission, inductively coupled plasma spectrometer (ICP-OES, Varian 720-ES with axial optics) at the GFZ HELGES laboratory (Table S2). Accuracy of measurements was evaluated by running aliquots of the geostandard "granite CRPG GA" (Govindaraju, 1995).

^{10}Be aliquots were spiked with 100–300 μg of the "phenakite" ^{9}Be carrier, which contains a ^{10}Be/^{9}Be ratio of $2.51 \pm 0.13 \times 10^{-15}$. Separation of ^{10}Be was carried out by anion and cation column separation and alkaline precipitation according to von Blanckenburg, Belshaw, and O'Nions (1996); von Blanckenburg et al. (2004). ^{10}Be/^{9}Be ratios were measured in BeO targets by accelerator mass spectrometry (AMS) at the Ion Beam Facility of the ETH Zurich relative to the in-house standard S2007N with a nominal ^{10}Be/^{9}Be value of 28.1×10^{-12} and at the Centre for Accelerator Mass Spectrometry at the University of Cologne (CologneAMS, relative to standards KN01-6-2 and KN01-5-3, with ^{10}Be/^{9}Be ratios of 5.35×10^{-13} and 6.32×10^{-12}, respectively). Results from both AMS facilities are consistent with a ^{10}Be half-life of 1.36 (±0.07) $\times 10^{6}$ year. Procedural blanks were subtracted and their errors were propagated into the reported concentrations (Table S2). All concentrations are relative to the initial weight of the sample. Replicates were analyzed for the Biobío, MUC1, and MUC3 samples (Tables S1 and S2, Figures 2 and 3).

The Biobío River outweighs the Lebu and Yani rivers in drainage area (Figure 1) and sediment export (Wittmann et al., 2017). Hence, we calculated a sediment-flux weighed average of the element compositions and Be-isotope concentrations using in situ ^{10}Be-derived sediment load (Wittmann et al., 2017).

4. Results

4.1. Elemental Composition

To detect changes in the sediment composition of the clay-sized fraction from the riverine to the marine realm, major and minor element abundances were analyzed (Figures 2 and S3; Table S1). Si content was not measured because the clay-sized fraction was digested using hydrofluoric acid (HF) leading to the loss of Si. All element concentrations increase from the riverine to marine clay-sized fraction roughly by a factor of two (Table S1, Figure S3).

Measured element concentrations are likely to be affected by the addition or removal of primary minerals (e.g., quartz) during sediment sorting encountered during transport. That enrichment by sorting occurred is shown by concentrations of Al, Ti, and Zr that all increase by a similar factor, with the lowest concentrations in the Biobío River, highest concentrations in the Lebu and Yani sediments, and intermediate concentrations in the marine samples (Figure 2a). As we are interested in concentration changes resulting from chemical processes, we removed such dilution/enrichment effects by normalizing all element concentrations to the concentration of Ti (Figure 2b), which can be considered as an immobile element in the terrestrial (Brimhall & Dietrich, 1987) and marine (Govin et al., 2012) realm. We further calculated an "increase factor" from the Ti-normalized element ratios by dividing the mean of the marine clay-sized fraction by the sediment-flux weighed mean of the river sediment of the clay-sized fraction (factor = 1: no increase, <1: decrease, >1: increase from the riverine to the marine clay-sized fraction, Figure 2c). The increase factors of the Ti-normalized element ratios from river sediment to marine surface sediment range between 1.4 and 0.8. Only ^{10}Be/Ti shows a high increase factor of 3.2.

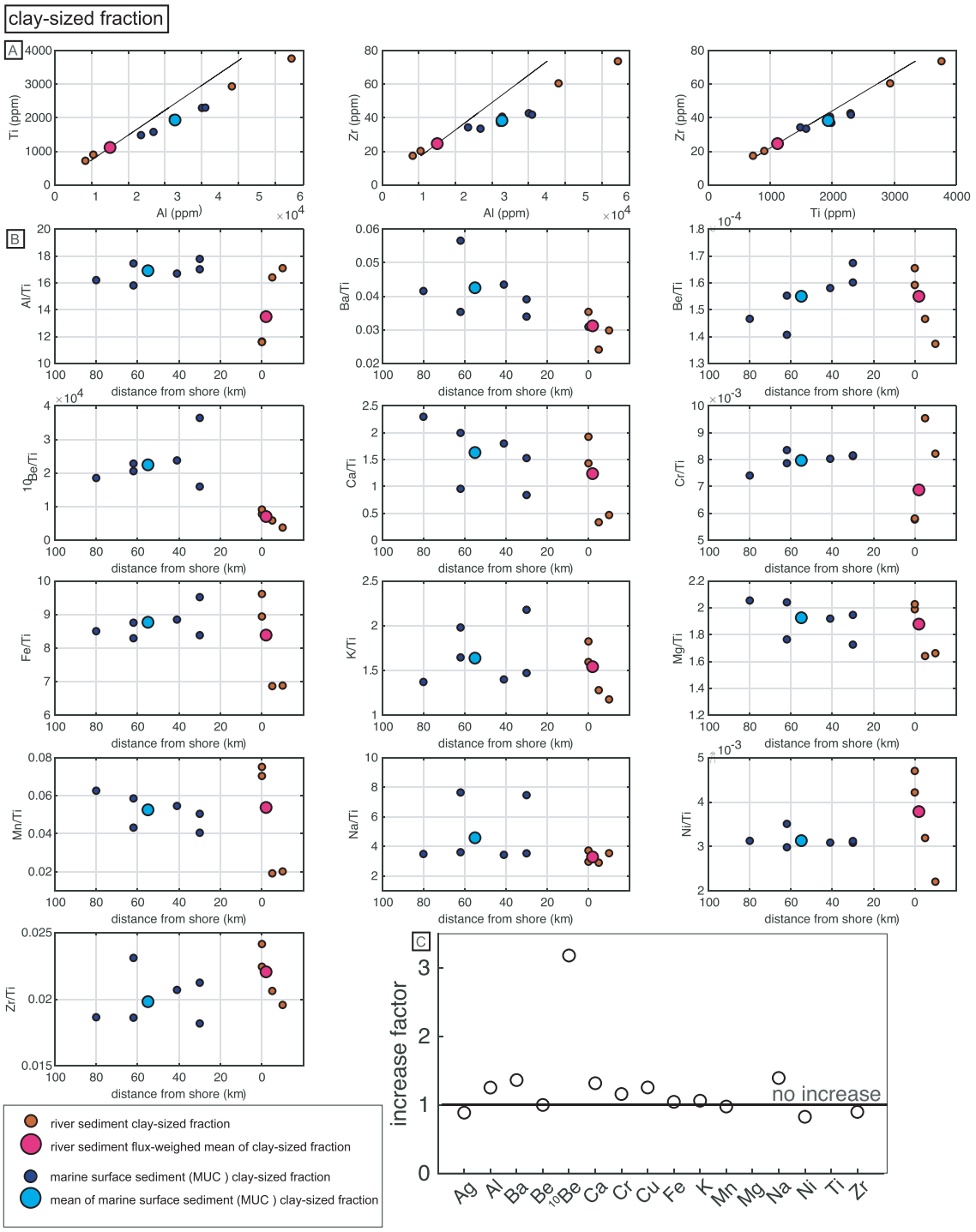

Figure 2. (a) Cross plots of the Al, Ti, and Zr concentrations of the clay-sized fraction of river and marine sediment, including their means. The solid black line shows the constant element ratio of the sediment-flux weighed mean of river samples. (b) Element and ^{10}Be concentrations normalized to the Ti concentration of the clay-sized fraction of river and marine sediment, respectively, including their means. Note that the sample order is arranged from west to east (see Figure 1), river-sediment samples plot on the far right, the distal MUC samples on the far left. Replicate measurements are shown for the Biobío, MUC1, and MUC3 samples. (c) The increase factor of Ti-normalized element ratios from the sediment-flux weighed mean of the river-sediment samples to the mean of the marine samples (clay-sized fraction only) derived by dividing the marine sediment mean X/Ti ratio by the sediment-flux weighed mean X/Ti ratio of the river sediment.

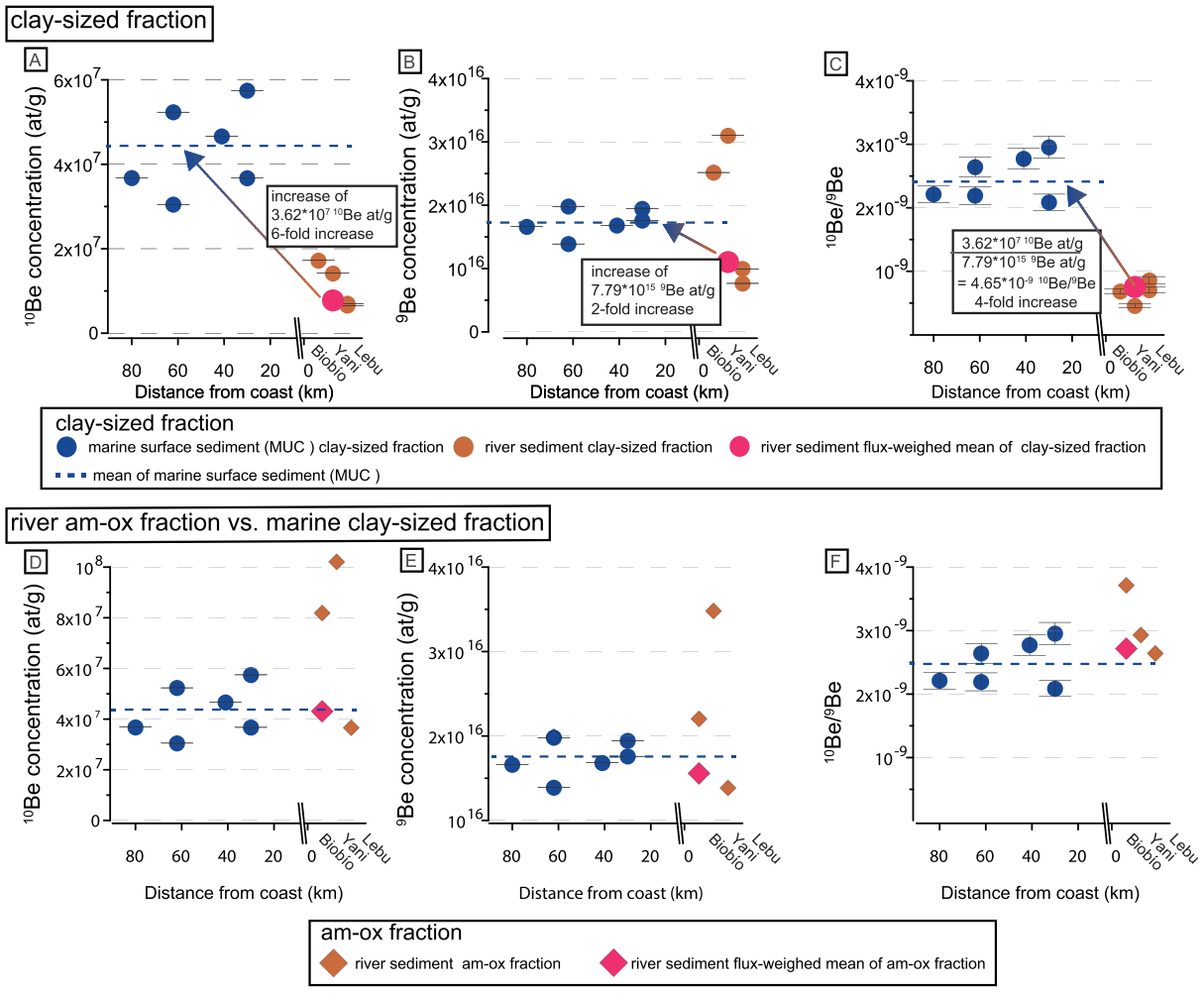

Figure 3. ^{10}Be and ^{9}Be concentrations for the (a–c) clay-sized fraction. Panels (d)–(f) show the comparison of the riverine am-ox fraction (from Wittmann et al., 2017) to the marine clay-sized fraction. Sample order is arranged from west to east (see Figure 1). All concentrations are reported relative to the initial weight of the sample. Measurement errors are smaller than the symbol size.

4.2. ^{10}Be, ^{9}Be, and ^{10}Be/^{9}Be ratios

The concentration of ^{10}Be in the marine clay-sized fraction ($[^{10}Be]_{clay\text{-}sized}$) increases on average sixfold when compared to the riverine counterpart (Figure 3a). $[^{10}Be]_{reac}$ is dependent on particle size whereas $^{10}Be/^{9}Be_{reac}$ is not (Wittmann et al., 2012). Grain size-dependence results from small particles providing increased specific surface area for ^{10}Be sorption. However, $[^{10}Be]_{clay\text{-}sized}$ should not depend on grain size as samples were chemically leached and thus no sorbed ^{10}Be remains. $[^{9}Be]_{clay\text{-}sized}$ shows a twofold increase from the terrestrial to marine realm (Figure 3b), as most other element concentrations (Table S1, Figure S3). Marine $^{10}Be/^{9}Be_{clay\text{-}sized}$ ratios show on average a fourfold increase when compared to the terrestrial $^{10}Be/^{9}Be_{clay\text{-}sized}$.

The average $[^{10}Be]_{clay\text{-}sized}$ of the marine surface sediment (Figure 3d) is equal to the sediment flux-weighed $[^{10}Be]_{am\text{-}ox}$ of the river-sediment samples (Wittmann et al., 2017). Most of the sediment flux-weighed $[^{10}Be]_{reac}$ is contained in the $[^{10}Be]_{am\text{-}ox}$ fraction, and hence, the x-ox fraction only carries a minor amount of ^{10}Be (Wittmann et al., 2017). [^{9}Be] shows more uniform concentrations from the river-sediment am-ox fraction to the marine clay-sized fraction (Figure 3e). Perhaps coincidentally, marine $^{10}Be/^{9}Be_{clay\text{-}sized}$ ratios are equivalent to the terrestrial $^{10}Be/^{9}Be_{am\text{-}ox}$ (Figure 3f, see section 5.1.4).

5. Discussion

5.1. Causes for the $^{10}Be/^{9}Be$ Increase From River to Marine Clay-Sized Sediment

Subsequently, we discuss possible causes for the increase in $[^{10}Be]_{clay\text{-}sized}$ and $^{10}Be/^{9}Be_{clay\text{-}sized}$ from the riverine to marine realm.

5.1.1. Distinct Sediment Provenance

Differences in terms of $[^{10}Be]_{clay\text{-}sized}$, $[^{9}Be]_{clay\text{-}sized}$, and $^{10}Be/^{9}Be_{clay\text{-}sized}$ between the riverine and marine sediment could simply be due to different provenance, for example if the sampled marine sediment was derived from a river basin located away from the three sampled rivers. However, we regard this possibility as unlikely. Given the presence of the southward-directed Gunther undercurrent, such sediment would be routed from the north and thus captured by the submarine canyon offshore the Biobío River mouth (Figure 1). Moreover, the ratios of insoluble element concentrations (such as Zr/Ti or Cr/Ti), which can also be used as sediment-source tracer, are similar between the riverine and marine clay-sized fraction (Figure 2). Mineralogic composition (Figure S1) does not indicate a major provenance change and silicate Nd and Sr isotopes remain roughly constant between the Biobío River and the marine MUC samples (Figure S2). Thus, our data hint toward a similar provenance for river and marine samples and we regard provenance effects as an unlikely cause for the observed differences in $[^{10}Be]_{clay\text{-}sized}$ and $^{10}Be/^{9}Be_{clay\text{-}sized}$.

5.1.2. Enrichment of Clay-Sized Marine Sediment in ^{10}Be Through Selective Loss of Primary Minerals

$[^{10}Be]_{clay\text{-}sized}$ increases sixfold from the riverine to marine samples whereas $[^{9}Be]_{clay\text{-}sized}$ increases twofold. Most element concentrations increase twofold from riverine to marine samples (Table S1, Figure S3), whereas most elemental ratios (excluding $^{10}Be/Ti$) are unchanged within scatter (Figure 2). We interpret this twofold increase of elemental concentrations to be due to the removal of virtually ^{10}Be-free primary minerals (e.g., quartz, Figure 2) from the riverine to marine clay-sized fraction by sediment-sorting processes (note that in situ $[^{10}Be]$ (Table S2) and $[^{9}Be]$ in quartz are negligible compared to meteoric $[^{10}Be]$; e.g., Wittmann et al., 2015).

The selective removal of primary minerals containing ^{9}Be (e.g., plagioclase, pyroxene; Grew, 2002) is unlikely as ^{9}Be increases twofold just like most other elements (Tables S1 and S2, Figure S3). Moreover, the Ca/Ti and Na/Ti ratios, which could be used as tracers for the abundance of plagioclase in the clay-sized fractions, are actually slightly higher in marine samples than in river samples (Figure 2). Hence, the loss of primary minerals does not suffice to explain the difference in $[^{10}Be]_{clay\text{-}sized}$ and $^{10}Be/^{9}Be_{clay\text{-}sized}$ between the riverine and marine clay-sized fractions but requires the formation of new phases in the ocean, incorporating Be with a high $^{10}Be/^{9}Be$ signature.

5.1.3. Authigenic Clay Formation

The high $^{10}Be/^{9}Be$ signature of the marine clay-sized fraction incorporated during land-ocean transfer cannot be attributed to any adsorbed or amorphous material, as these phases were removed during chemical leaching prior to separation of the clay-sized fraction. As a consequence, the most likely candidate for the incorporation of Be between river and marine sediment is the formation of authigenic clays. The processes responsible for the formation of authigenic silicate phases in the marine realm are still somewhat enigmatic. Although in continental shelf and deep-sea sediments, the bulk of the clay-sized fraction is detrital (Kastner, 1981), the neoformation of authigenic clays in the marine realm can occur by low-temperature interaction between amorphous hydr (oxides) (am-ox fraction) and biogenic amorphous silica. Authigenic clay-mineral formation requires sources of Al which is provided by the dissolution of unstable, amorphous Al (hydr-)oxides or other highly weathered aluminosilicates (e.g., Mackenzie & Garrels, 1966) or volcanic ashes (Dunlea et al., 2017) and Si derived from biogenic opaline silica (e.g., Ehlert et al., 2016; Rahman et al., 2016). Mackenzie and Garrels (1966) first suggested a general chemical reaction of the form

$$\begin{aligned}&\text{amorphous Al–silicate and reactive Al}\,(OH)_3 + HCO_3^- + SiO_2 + \text{cations}\\&\quad = \text{cation Al–silicate} + CO_2 + H_2O.\end{aligned}$$

Recent studies have shown that reverse weathering reactions majorly affect the clay composition of sediments along continental margins (Baldermann et al., 2015; Dunlea et al., 2017; Ehlert et al., 2016; Rahman et al., 2016; Santiago Ramos et al., 2018; Wallmann et al., 2008). Moreover, Tosca et al. (2016)

demonstrated that authigenic clays can form from dissolved constituents, not requiring Al or precursor phases.

Our observations of the Be isotope composition of sediments onshore and offshore the Chilean coast lend support to these recent findings: $[^{10}Be]_{clay\text{-}sized}$ increases sixfold from the riverine to marine realm (Figure 3a), whereas the quartz-removal effect by sediment sorting on element-concentration increase amounts only to a factor of approximately two (Figure S3). Hence, additional ^{10}Be is incorporated in the marine clay-sized fraction. Indeed, Be with a high Pacific open-ocean (dissolved) $^{10}Be/^{9}Be$ ratio of ~1.1×10^{-7} (Kusakabe et al., 1987) could be incorporated into authigenic phases through its scavenging into silica frustules by diatoms or radiolarians in the water column (Bourlès et al., 1989; Frank et al., 1995; Lal et al., 2006). Subsequent dissolution of this biogenic opaline silica fuels the formation of authigenic clays during diagenesis in the sediment (e.g., Ehlert et al., 2016; Rahman et al., 2016).

It is likely that the clay-sized fraction retrieves its additional ^{10}Be from that same seawater source as the amorphous hydroxide (am-ox) fraction previously measured by Wittmann et al. (2017). The am-ox fraction shows a tenfold increase in [^{10}Be] and $^{10}Be/^{9}Be$ ratio from river to ocean sediment (Figure 3), whereas the increase in the clay-sized fraction is fourfold. Both types of $^{10}Be/^{9}Be$ ratios are thus thought to reflect mixing between initial terrigenous Be and added seawater Be.

However, we also note that the average marine $[^{10}Be]_{clay\text{-}sized}$ and $(^{10}Be/^{9}Be)_{clay\text{-}sized}$ (2.47×10^{-9}) are similar to that of the riverine flux-weighed mean of the am-ox fraction ($^{10}Be/^{9}Be = 2.73 \times 10^{-9}$, flux-weighed mean) (Figures 3d and 3f, Table S2). Given this similarity, the source of added Be to marine clays could potentially stem from the riverine am-ox fraction. In this case, the transformation of the riverine am-ox fraction into marine authigenic clays might occur during early diagenesis, when the am-ox phases are reduced and hence dissolved below a sedimentary redox front. This reduction would entail release of their Be into the pore water, which is taken up by authigenic clays. The authigenic phase would then record the terrestrial river basins' denudation rate (von Blanckenburg et al., 2012). This process would, however, require complete overprinting of the $(^{10}Be/^{9}Be)_{clay\text{-}sized}$ inherited from the terrigenous realm, which we consider as unlikely. Furthermore, it seems rather unlikely that the $(^{10}Be/^{9}Be)_{clay\text{-}sized}$ increases due to addition of Be from the river am-ox fraction, whereas the marine $(^{10}Be/^{9}Be)_{am\text{-}ox}$ has increased from Be addition from seawater (Wittmann et al., 2017). Hence, the similarity between the riverine $(^{10}Be/^{9}Be)_{am\text{-}ox}$ and the marine $(^{10}Be/^{9}Be)_{clay\text{-}sized}$ at our sites is more likely to be pure coincidence. Regardless of the exact mechanism by which $^{10}Be/^{9}Be$ ratios increase in the clay-sized fraction, our Be-isotope based observations reflect the formation of authigenic phases in marine sediments during early diagenesis. $^{10}Be/^{9}Be$ ratios thus appear as a sensitive proxy of these processes.

5.2. Be Isotopes in Marine Clay-Sized Sediment: A Proxy for Authigenic Clay Formation or for Terrigenous Denudation?

Using a simple mixing model where the sediment flux-weighed mean $^{10}Be/^{9}Be$ of the riverine clays is mixed with clay that incorporated Pacific dissolved $^{10}Be/^{9}Be$ (from Kusakabe et al., 1987), we calculate that <2% of such pure marine authigenic clay would suffice to explain the observed marine mean $(^{10}Be/^{9}Be)_{clay\text{-}sized}$ (Figure S4). This end-member calculation suggests that such low amounts of authigenic clays involved make it very difficult to detect neoformation of clays during marine diagenesis with "classical" analytical methods such as XRD or chemical composition of sediments. In contrast, the markedly different $^{10}Be/^{9}Be$ ratios between terrestrially derived and ocean Be pools make Be isotopes a very sensitive tracer of marine authigenic clay formation, and more generally of reverse weathering processes. The proxy can theoretically be applied to all ocean basins where the terrestrial and ocean $^{10}Be/^{9}Be$ signatures are known and markedly different. However, ^{10}Be undergoes radioactive decay. Hence, the proxy cannot be used to reconstruct the role of reverse weathering in deep time, but rather track these processes during recent Earth history (last ~13 Ma) with possible implications for the past. We also note that it is not trivial to translate the amount of authigenic clays produced, as constrained by this proxy, to the amount of CO_2 released during reverse weathering as this CO_2-flux would depend on the amount and valency of the major cations involved in the reaction (e.g., Isson & Planavsky, 2018).

Because the terrestrial riverine $^{10}Be/^{9}Be$ ratio is altered within both the am-ox and clay-sized fraction when the river sediment is exposed to seawater, the terrestrial $^{10}Be/^{9}Be$ signal cannot be recovered from marine

sediment. Therefore, terrestrial denudation rates from river catchments that feed the marine sample locations cannot be derived to date. Such endeavor would first require development of a clay-separation procedure that separates pure terrigenous clay from marine clay-sized sediment, which is still missing for the moment. Such regional denudation rate would differ from the global denudation proxy introduced by Willenbring and von Blanckenburg (2010) and further developed by von Blanckenburg and Bouchez (2014), where the formerly dissolved, ocean basin-wide, well-mixed $^{10}Be/^{9}Be$ is precipitated in ferromanganese crusts from ocean water that then records global denudation integrated over 10^5 years.

6. Conclusions

We observed a fourfold increase in $^{10}Be/^{9}Be$ isotope ratios of Be in the clay-sized fraction of marine sediments when compared to the $^{10}Be/^{9}Be$ ratios of the corresponding terrestrial riverine source. This increase, which is due to high meteoric ^{10}Be concentrations in seawater, requires the formation of a new silicate phase in marine surface sediment. Results from a previous study using the same sample set similarly suggest that $^{10}Be/^{9}Be$ ratios of marine authigenic iron-oxy-hydroxide phases comprise a mixture of a terrestrial and an oceanic component (Wittmann et al., 2017). In both cases, the seawater-derived ^{10}Be is incorporated into marine authigenic phases in which dissolved Be features a $^{10}Be(meteoric)/^{9}Be$ ratio that is almost two orders of magnitude higher than the ratio of the terrigenous riverine source. Thus, even though we removed authigenic reactive phases prior to clay separation, the fourfold increase in $^{10}Be/^{9}Be$ ratios in clay-sized sediment shows the terrestrial $^{10}Be/^{9}Be$ isotope signal is not preserved in the marine clay-sized fraction. If this obliteration of the terrigenous $^{10}Be/^{9}Be$ ratio in the marine realm is a general feature, river-basin denudation rates cannot be inferred from Be isotopes in clay.

If, however, the observed ^{10}Be increase occurs in the marine realm, incorporation of seawater-derived ^{10}Be within near-surface sediment may occur through the dissolution of marine biogenic opaline silica (a high-$^{10}Be/^{9}Be$ phase as its Be incorporates the open-ocean ratio). Opaline silica serves as a Si-source for the precipitation of marine authigenic clays via reverse-weathering reactions. The $^{10}Be/^{9}Be$ isotope ratio in clay-sized marine sediment thus bears potential as a high-sensitivity proxy for the formation of marine authigenic clays. Reverse weathering has been recently recognized as an important controlling factor of the ocean-alkalinity balance that impacts atmospheric CO_2 and, thus, global climate (Dunlea et al., 2017; Isson & Planavsky, 2018). Hence, such a highly sensitive proxy for authigenic clay formation is essential to quantify these processes.

Acknowledgments
This project was supported by DFG grant WI 3874/2-1 and BE 5070/2-1 (to H. Wittmann and A. Bernhardt). We thank C. Günter and D. Kauschus for XRD-support and D. Melnick and A. Tassara for river-sediment sampling. We thank S. Binnie and S. Heinze (Cologne University) for AMS measurements. L. Faure is acknowledged for analytical support, part of which was supported by the IPGP multidisciplinary program PARI and by Paris-IdF region SESAME grant 12015903. We thank reviewers T. Isson and Q. Simon for their constructive criticism. Data are stored at the GFZ Data Services https://doi.org/10.5880/fidgeo.2020.009.

References

Baldermann, A., Warr, L. N., Letofsky-Papst, I., & Mavromatis, V. (2015). Substantial iron sequestration during green-clay authigenesis in modern deep-sea sediments. *Nature Geoscience*, *8*(11), 885–889. https://doi.org/10.1038/ngeo2542

Bernhardt, A., Hebbeln, D., Regenberg, M., Lückge, A., & Strecker, M. R. (2016). Shelfal sediment transport by an undercurrent forces turbidity current activity during high sea level, Chile continental margin. *Geology*, *44*(4), 295–298. https://doi.org/10.1130/G37594.1

Bernhardt, A., Melnick, D., Jara-Muñoz, J., Argandoña, B., González, J., & Strecker, M. R. (2015). Controls on submarine canyon activity during sea-level highstands: The Biobío canyon system offshore Chile. *Geosphere*, *11*(4), 1–30. https://doi.org/10.1130/GES01063.1

Bourlès, D., Raisbeck, G., & Yiou, F. (1989). ^{10}Be and ^{9}Be in marine sediments and their potential for dating. *Geochimica et Cosmochimica Acta*, *53*(2), 443–452.

Brimhall, G. H., & Dietrich, W. E. (1987). Constitutive mass balance relations between chemical composition, volume, density, porosity, and strain in metasomatic hydrochemkai systems: Results on weathering and pedogenesis. *Geochimica et Cosmochimica Acta*, *51*(4), 567–587.

Brown, E. T., Edmond, J. M., Raisbeck, G. M., Bourlès, D. L., Yiou, F., & Measures, C. I. (1992). Beryllium isotope geochemistry in tropical river basins. *Geochimica et Cosmochimica Acta*, *56*(4), 1607–1624. https://doi.org/10.1016/0016-7037(92)90228-B

Brown, E. T., Measures, C. I., Edmond, J. M., Bourlès, D. L., Raisbeck, G. M., & Yiou, F. (1992). Continental inputs of beryllium to the oceans. *Earth and Planetary Science Letters*, *114*(1), 101–111. https://doi.org/10.1016/0012-821X(92)90154-N

Carcaillet, J., Bourlès, D. L., Thouveny, N., & Arnold, M. (2004). A high resolution authigenic $^{10}Be/^{9}Be$ record of geomagnetic moment variations over the last 300 ka from sedimentary cores of the Portuguese margin. *Earth and Planetary Science Letters*, *219*(3–4), 397–412. https://doi.org/10.1016/S0012821X03007027

Christl, M., Strobl, C., & Mangini, A. (2003). Beryllium-10 in deep-sea sediments: A tracer for the Earth's magnetic field intensity during the last 200,000 years. *Quaternary Science Reviews*, *22*(5-7), 725–739. https://doi.org/10.1016/S0277-3791(02)00195-6

Dunlea, A. G., Murray, R. W., Santiago Ramos, D. P., & Higgins, J. A. (2017). Cenozoic global cooling and increased seawater Mg/Ca via reduced reverse weathering. *Nature Communications*, *8*(1), 1, 844–6. https://doi.org/10.1038/s41467-017-00853-5

Ehlert, C., Doering, K., Wallmann, K., Scholz, F., Sommer, S., Grasse, P., et al. (2016). Stable silicon isotope signatures of marine pore waters—Biogenic opal dissolution versus authigenic clay mineral formation. *Geochimica et Cosmochimica Acta*, *191*, 102–117. https://doi.org/10.1016/j.gca.2016.07.022

Foster, M. (1953). Geochemical studies of clay minerals III. The determination of free silica and free alumina in montmorillonites. *Geochimica et Cosmochimica Acta*, *3*, 143–154.

Frank, M., Eisenhauer, A., Bonn, W. J., Walter, P., Grobe, H., Kubik, P. W., et al. (1995). Sediment redistribution versus paleoproductivity change: Weddell Sea margin sediment stratigraphy and biogenic particle flux of the barium profiles. *Earth and Planetary Science Letters*, *136*(95), 559–573.

Govin, A., Holzwarth, U., Heslop, D., Ford Keeling, L., Zabel, M., Mulitza, S., et al. (2012). Distribution of major elements in Atlantic surface sediments (36°N–49°S): Imprint of terrigenous input and continental weathering. *Geochemistry, Geophysics, Geosystems*, *13*, Q01013. https://doi.org/10.1029/2011GC003785

Govindaraju, K. (1995). Working values with confidence limits for twenty-six CRPG, ANRT and IWG-GIT geostandards. *Geostandards Newsletter*, *19*, 1–32.

Grew, E. S. (2002). Beryllium in metamorphic environments (emphasis on aluminous compositions). *Reviews in Mineralogy and Geochemistry*, *50*(1), 487–549.

Hebbeln, D., & Shipboard Scientists (2001). PUCK: Report and preliminary results of R/V Sonne cruise SO156, Valparaiso (Chile)–Talcahuano (Chile), March 29–May 14, 2001.

Igel, H., & von Blanckenburg, F. (1999). Lateral mixing and advection of reactive isotopetracers in ocean basins: Numerical modeling. *Geochemistry, Geophysics, Geosystems*, *1*(1). https://doi.org/10.1029/1999GC000003

Isson, T. T., & Planavsky, N. J. (2018). Reverse weathering as a long-term stabilizer of marine pH and planetary climate. *Nature*, *560*(7719), 471–475. https://doi.org/10.1038/s41586-018-0408-4

Kastner, M. (1981). Authigenic silicates in deep-sea sediments: Formation and diagenesis. In E. Emiliani (Ed.), *The Sea* (pp. 915–988). New York: Wiley.

Knudsen, M. F., Henderson, G. M., Frank, M., Mac Niociall, C., & Kubik, P. W. (2008). In-phase anomalies in Beryllium-10 production and palaeomagnetic field behaviour during the Iceland Basin geomagnetic excursion. *Earth and Planetary Science Letters*, *265*(3–4), 588–599. https://doi.org/10.1016/j.epsl.2007.10.051

Kusakabe, M., & Ku, T. L. (1984). Incorporation of Be isotopes and other trace metals into marine ferromanganese deposits. *Geochimica et Cosmochimica Acta*, *48*(11), 2187–2193. https://doi.org/10.1016/0016-7037(84)90215-1

Kusakabe, M., Ku, T. L., Southon, J. R., Vogel, J. S., Nelson, D. E., Measures, C. I., & Nozaki, Y. (1987). Distribution of ^{10}Be and ^{9}Be in the Pacific Ocean. *Earth and Planetary Science Letters*, *82*(3-4), 231–240. https://doi.org/10.1016/0012-821X(87)90198-1

Lal, D., Charles, C., Vacher, L., Goswami, J., Jull, A., McHargue, L., & Finkel, R. (2006). Paleo-ocean chemistry records in marine opal. Implications for fluxes of trace elements, cosmogenic nuclides (10Be and 26Al), and biological productivity. *Geochimica et Cosmochimica Acta*, *70*(13), 3275–3289. https://doi.org/10.1016/j.gca.2006.04.004

Mackenzie, F. T., & Garrels, R. M. (1966). Chemical mass balance between rivers and oceans. *American Journal of Science*, *264*, 507–525.

Mackin, J. E., & Aller, R. C. (1984). Dissolved Al in sediments and waters of the East China Sea: Implications for authigenic mineral formation. *Geochimica et Cosmochimica Acta*, *48*(2), 281–297. https://doi.org/10.1016/0016-7037(84)90251-5

Mackin, J. E., & Aller, R. C. (1986). The effects of clay mineral reactions on dissolved Al distributions in sediments and waters of the Amazon continental shelf. *Continental Shelf Research*, *6*(1–2), 245–262. https://doi.org/10.1016/0278-4343(86)90063-4

Ménabréaz, L., Bourlès, D. L., & Thouveny, N. (2012). Amplitude and timing of the Laschamp geomagnetic dipole low from the global atmospheric ^{10}Be overproduction: Contribution of authigenic ^{10}Be/^{9}Be ratios in west equatorial Pacific sediments. *Journal of Geophysical Research*, *117*, B11101. https://doi.org/10.1029/2012JB009256

Ménabréaz, L., Thouveny, N., Bourlès, D. L., & Vidal, L. (2014). The geomagnetic dipole moment variation between 250 and 800 ka BP reconstructed from the authigenic ^{10}Be/^{9}Be signature in West Equatorial Pacific sediments. *Earth and Planetary Science Letters*, *385*, 190–205. https://doi.org/10.1016/j.epsl.2013.10.037

Michalopoulos, P., & Aller, R. C. (1995). Rapid clay mineral formation in Amazon delta sediments: Reverse Weathering and Oceanic Elemental Cycles. *Science*, *270*(5236), 614–617.

Michalopoulos, P., & Aller, R. C. (2004). Early diagenesis of biogenic silica in the Amazon delta: Alteration, authigenic clay formation, and storage. *Geochimica et Cosmochimica Acta*, *68*(5), 1061–1085. https://doi.org/10.1016/j.gca.2003.07.018

Rahman, S., Aller, R. C., & Cochran, J. K. (2016). Cosmogenic ^{32}Si as a tracer of biogenic silica burial and diagenesis. Major deltaic sinks in the silica cycle. *Geophysical Research Letters*, *43*, 7124–7132. https://doi.org/10.1002/2016GL069929

Rugenstein, J. K. C., Ibarra, D. E., & Von Blanckenburg, F. (2019). Neogene cooling driven by land surface reactivity rather than increased weathering fluxes. *Nature*, *571*(7763), 99–102. https://doi.org/10.1038/s41586-019-1332-y

Santiago Ramos, D. P., Morgan, L. E., Lloyd, N. S., & Higgins, J. A. (2018). Reverse weathering in marine sediments and the geochemical cycle of potassium in seawater: Insights from the K isotopic composition (41K/39K) of deep-sea pore-fluids. *Geochimica et Cosmochimica Acta*, *236*, 99–120. https://doi.org/10.1016/j.gca.2018.02.035

Sauer, D., Saccone, L., Conley, D. J., Herrmann, L., & Sommer, M. (2006). Review of methodologies for extracting plant-available and amorphous Si from soils and aquatic sediments. *Biogeochemistry*, *80*(1), 89–108. https://doi.org/10.1007/s10533-005-5879-3

Scholz, F., Hensen, C., Schmidt, M., & Geersen, J. (2013). Submarine weathering of silicate minerals and the extent of pore water freshening at active continental margins. *Geochimica et Cosmochimica Acta*, *100*, 200–216. https://doi.org/10.1016/j.gca.2012.09.043

Segl, M., Mangini, A., Bonani, G., Hofmann, H. J., Nessi, M., Suter, M., et al. (1984). ^{10}Be-dating of a manganese crust from Central North Pacific and implications for ocean palaeocirculation. *Nature*, *309*(5968), 540–543. https://doi.org/10.1038/309540a0

Simon, Q., Bourlès, D. L., Thouveny, N., Horng, C. S., Valet, J. P., Bassinot, F., & Choy, S. (2018). Cosmogenic signature of geomagnetic reversals and excursions from the Réunion event to the Matuyama–Brunhes transition (0.7–2.14 Ma interval). *Earth and Planetary Science Letters*, *482*, 510–524. https://doi.org/10.1016/j.epsl.2017.11.021

Simon, Q., Thouveny, N., Bourles, D. L., Nuttin, L., Hillaire-Marcel, C., & St-Onge, G. (2016). Authigenic ^{10}Be/^{9}Be ratios and ^{10}Be-fluxes (^{230}Th$_{xs}$-normalized) in central Baffin Bay sediments during the last glacial cycle Paleoenvironmental implications. *Quaternary Science Reviews*, *140*, 142–162. https://doi.org/10.1016/j.quascirev.2016.03.027

Simon, Q., Thouveny, N., Bourlès, D. L., Valet, J. P., Bassinot, F., Ménabréaz, L., et al. (2016). Authigenic ^{10}Be/^{9}Be ratio signatures of the cosmogenic nuclide production linked to geomagnetic dipole moment variation since the Brunhes/Matuyama boundary. *Journal of Geophysical Research: Solid Earth*, *121*, 7716–7741. https://doi.org/10.1002/2016JB013335

Tessier, A., Campbell, P. G. C., & Bisson, M. (1979). Sequential extraction procedure for the speciation of particulate trace metals. *Analytical Chemistry*, *51*(7), 844–851. https://doi.org/10.1021/ac50043a017

Tosca, N. J., Guggenheim, S., & Pufahl, P. K. (2016). An authigenic origin for Precambrian greenalite: Implications for iron formation and the chemistry of ancient seawater. *Bulletin of the Geological Society of America*, *128*(3–4), 511–530. https://doi.org/10.1130/B31339.1

Valletta, R. D., Willenbring, J. K., Passchier, S., & Elmi, C. (2018). ^{10}Be/^{9}Be ratios reflect Antarctic Ice Sheet freshwater discharge during Pliocene warming. *Paleoceanography and Paleoclimatology*, *33*, 934–944. https://doi.org/10.1029/2017PA003283

von Blanckenburg, F., Belshaw, N. S., & O'Nions, R. K. (1996). Separation of ^{9}Be and cosmogenic ^{10}Be from environmental materials and SIMS isotope dilution analysis. *Chemical Geology*, *129*(1–2), 93–99. https://doi.org/10.1016/0009-2541(95)00157-3

von Blanckenburg, F., & Bouchez, J. (2014). River fluxes to the sea from the ocean's ^{10}Be/^{9}Be ratio. *Earth and Planetary Science Letters*, *387*, 34–43. https://doi.org/10.1016/j.epsl.2013.11.004

von Blanckenburg, F., Bouchez, J., Ibarra, D. E., & Maher, K. (2015). Stable runoff and weathering fluxes into the oceans over Quaternary climate cycles. *Nature Geoscience*, *8*(July), 538–543. https://doi.org/10.1038/ngeo2452

von Blanckenburg, F., Bouchez, J., & Wittmann, H. (2012). Earth surface erosion and weathering from the ^{10}Be (meteoric)/^{9}Be ratio. *Earth and Planetary Science Letters*, *352*, 295–305.

von Blanckenburg, F., Hewawasam, T., & Kubik, P. W. (2004). Cosmogenic nuclide evidence for low weathering and denudation in the wet, tropical highlands of Sri Lanka. *Journal of Geophysical Research*, *109*, F03008. https://doi.org/10.1029/2003JF000049

von Blanckenburg, F., O'Nions, R. K., Belshaw, N. S., Gibb, A., & Hein, J. R. (1996). Global distribution of beryllium isotopes in deep ocean water as derived from Fe-Mn crusts. *Earth and Planetary Science Letters*, *141*(1–4), 213–226. https://doi.org/10.1016/0012-821X(96)00059-3

Wallmann, K., Aloisi, G., Haeckel, M., Tishchenko, P., Pavlova, G., Greinert, J., et al. (2008). Silicate weathering in anoxic marine sediments. *Geochimica et Cosmochimica Acta*, *72*(12), 2895–2918. https://doi.org/10.1016/j.gca.2008.03.026

Willenbring, J. K., & von Blanckenburg, F. (2010). Long-term stability of global erosion rates and weathering during late-Cenozoic cooling. *Nature*, *465*(7295), 211–214. https://doi.org/10.1038/nature09044

Wittmann, H., von Blanckenburg, F., Bouchez, J., Dannhaus, N., Naumann, R., Christl, M., & Gaillardet, J. (2012). The dependence of ^{10}Be concentrations on particle size in Amazon River sediment and the extraction of reactive ^{10}Be/^{9}Be ratios. *Chemical Geology*, *318–319*, 126–138.

Wittmann, H., von Blanckenburg, F., Dannhaus, N., Bouchez, J., Gaillardet, J., Guyot, J. L., et al. (2015). A test of the cosmogenic ^{10}Be (meteoric)/^{9}Be proxy for simultaneously determining basin-wide erosion rates, denudation rates, and the degree of weathering in the Amazon basin. *Journal of Geophysical Research: Earth Surface*, *120*, 2498–2528. https://doi.org/10.1002/2014JF003270.Received

Wittmann, H., von Blanckenburg, F., Mohtadi, M., Christl, M., & Bernhardt, A. (2017). The competition between coastal trace metal fluxes and oceanic mixing from the ^{10}Be/^{9}Be ratio: Implications for sedimentary records. *Geophysical Research Letters*, *44*, 8443–8452. https://doi.org/10.1002/2017GL074259